International Journal of
MATERIALS RESEARCH

Zeitschrift für METALLKUNDE

A Applied

Du Xinghao[a,b], Wu Baolin[b], J. C. Huang[a]
[a] Institute of Materials Science and Engineering, Center for Nanoscience and Nanotechnology, National Sun Yat-San University, Kaohsiung, Taiwan, China
[b] Department of Materials Engineering, Shenyang Institute of Aeronautical Engineering, Shenyang, P.R.China

Superplastic deformation behavior of a spray-deposited eutectic NiAl/Cr(Mo) alloy doped with Dy

The tensile deformation behavior at elevated temperatures and the associated mechanisms are investigated for hot isostatic pressed (HIP) NiAl-28Cr-5.9Mo-0.1Dy fabricated through spray forming. Superplasticity is observed at above 1323 K under an initial strain rate lower than 10^{-3} s^{-1} with an m value of 0.5. The activation energies for superplastic flow are found to be half of that for self-diffusion in NiAl. The grain boundary sliding between NiAl and adjacent NiAl or Cr(Mo) grains with local range accommodation, i.e., dynamic recovery, is suggested to be responsible for the superplastic deformation of the alloy.

Keywords: Spray forming; Ni-28Cr-6 Mo (Dy) alloy; Superplasticity; Grain boundary sliding

1. Introduction

The B2 type intermetallic compound NiAl is an attractive matrix for high temperature structural materials to replace nickel-based superalloys due to its high melting point, low density, good thermal conductivity and good oxidation resistance [1, 2]. However, poor damage tolerance at ambient temperatures and inadequate strength at high temperatures have prevented its commercial application. It has been found that these shortcomings can be improved significantly by the fabrication of NiAl-based eutectic composites involving a refractory metal as a reinforcing phase, and the alloy NiAl-28Cr-6Mo displays the most promising properties so far [3, 4]. However, these materials are difficult to form by conventional processing routes due to the high elastic modulus and high melting points. Fortunately, it is known that superplasticity can provide the possibility of high-temperature deformation processing of these brittle materials and has the advantages of sharper formability with better dimensional accuracy [5].

Superplasticity has been reported on B2 type intermetallic compounds NiAl alloys [6–12]. Single-phase NiAl with coarse grains (average grain size larger than 200 μm) exhibits superplastic deformation under certain conditions and continuous dynamic recrystallization is suggested to be the mainly operative mechanism [6–9]. On the other hand, grain boundary sliding (GBS) is suggested to be responsible for the superplasticity for multiphase NiAl alloys with fine microstructure [10–12]. However, the preparation of fine structures for NiAl alloys is complex and costly, because the extrusion temperature of NiAl ingots is usually needed to be higher than 1000 °C. The purpose of the present study is to investigate the superplastic behavior of the NiAl/Cr(Mo) alloy fabricated via the spray forming method. Spray forming has an advantage over casting and hot extrusion since it consists of atomization and consolidation in a single step, such that complex manufacturing steps used for the casting and hot extrusion processing method can be eliminated. For this reason mass production is possible and so production costs can be reduced.

MK_mk101449 – 5.1.07/druckhaus köthen

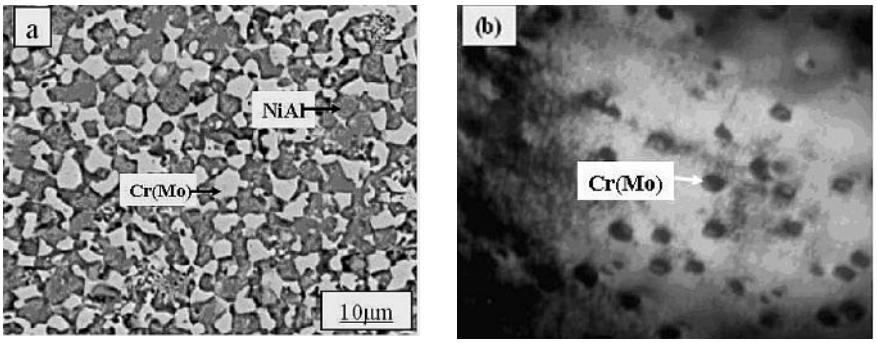

Fig. 1. SEM image of the as-HIPped microstructure (a) and TEM image of the NiAl matrix (b) of the alloy.

2. Experimental procedure

The nominal NiAl-28Cr-5.9Mo-0.1Dy (at.%) alloy, using high-purity metal elements as starting materials, was induction melted under vacuum conditions and drop cast into a cylindrical chill mold. Then the master alloy was atomized at 1600 °C and sprayed onto a water-cooled copper substrate in an Ar environment. After that, the obtained materials were condensed by hot isostatic pressing (HIP) at 1200 °C/100 MPa for 4 h and then homogenized by annealing for 24 h at 1000 °C. Flat tensile specimens, having a gage section $2 \times 2.5 \times 16$ mm^3, were electro-discharge machined. Tensile tests were carried out using a Shimadzu AG-25KNE testing machine up to 1373 K. Tensile specimens were heated to the deformation temperature at a heating rate of 15 K min^{-1} and maintained at temperature with an accuracy of ±1 K during deformation under the condition of constant crosshead speed. Tensile loads were automatically recorded by a connected computer, true stress–true strain curves were drawn from data recorded by the computer under assumption of volume conservation according to the method employed by Oomori et al. [13]. In some cases, deformation was interrupted at a given elongation and specimens were water quenched as quickly as possible. The specimens for SEM microscopy were etched in a solution of 5 g $FeCl_3$ + 15 ml HCl + 65 ml CH_3COOH. The foils for TEM observation were taken from the center part of the gauge section and prepared by ion milling using argon ion after mechanical polishing to 30 μm, and then the samples were examined in a Philips TEM 420 analytical electron microscope operated at 150 kV.

3. Experimental Results

3.1. The as-HIPed structure

A typical SEM micrograph showing the microstructural morphology of the alloy obtained after HIPping is shown in Fig. 1a. It finds that a two phase structure consisting of equiaxed NiAl and Cr(Mo) grains has been formed. Quantitative analysis of the microstructure indicated that equiaxed grains have an average grain size of about 4–5 μm for both phases, and the volume fraction of the Cr(Mo) phase is about 0.35. Since the materials used in this experiment were prepared by thermomechanical processing of ingots, grain boundaries and phase boundaries would not be contaminated. It is interesting that a certain amount of fine α-Cr(Mo) phase granules are dispersed in the primary NiAl matrix (Fig. 1b), which is clearly beneficial for the alloy to prevent the grains coarsening excessively at high temperatures.

3.2. The tensile properties

Elongations defined as total strain to failure are evaluated for different testing parameters. Concerning the strain rate dependence of the alloys, it is observed that the maximum elongation (i. e. optimum condition of superplasticity) is related to an initial strain rate of 1.04×10^{-4} s^{-1} at 1373 K. Figure 2 displays an image of specimens tested at 1323 K and 1373 K under the various strain rates. The results reveal that these specimens deform almost uniformly to fracture without obvious necking, which is similar to the character of superplastic deformation of many metallic alloys [14, 15]. However, the specimen for 1373 K under the 1.04×10^{-3} s^{-1} in Fig. 2 shows necking, which may be caused by the unevenly distribution of temperature in the tensile machine.

True stress–true strain curves are drawn from data recorded by the computer under the assumption of volume conservation according to the method employed by Oomori et al. [14]. Since all the tests were conducted under the condition of constant crosshead speed, the strain rate was not constant. Therefore, the curves of flow stress versus strain may be somewhat different from those under the condition of constant strain rate.

Based on the widely used stress versus strain relation in superplasticity, i. e. $\sigma = K\dot{\varepsilon}^m$ where k is a constant, a correlation to transform the stress at non-constant strain rate to that at constant strain rate is developed as

$$\sigma_{c\varepsilon} = \sigma_{cv} e^{m(\varepsilon - 0.002)} \quad (1)$$

$\sigma_{c\varepsilon}$ is the stress under the condition of constant strain rate, 0.002 is true strain corresponding to yielding point, σ_{cv} is the stress under the condition of constant cross head speed. According to the above correlation, the curves of flow stress versus strain under different deformation speeds were

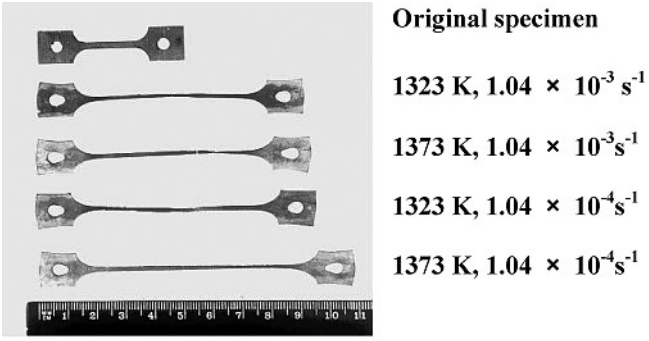

Fig. 2. Macrographs of fracture specimens of NiAl-30.9Cr-3Mo-0.1Dy alloy under different temperatures and strain rates.

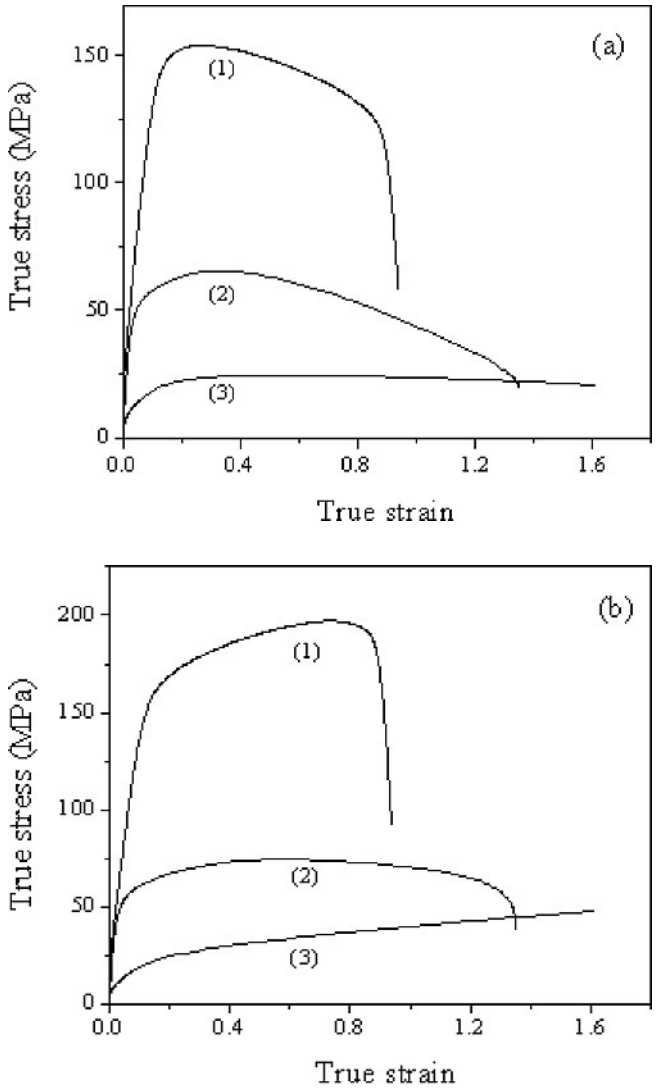

Fig. 3. True stress–true strain curves for the tested alloy under constant crosshead speed (a) and constant strain rate (b) at 1323 K. ((1): $5.02 \times 10^{-3}\ s^{-1}$; (2): $1.04 \times 10^{-3}\ s^{-1}$; (3): $1.04 \times 10^{-4}\ s^{-1}$).

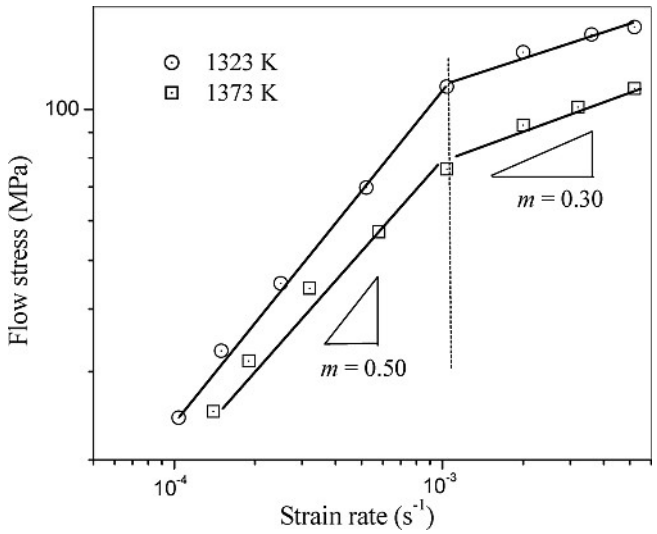

Fig. 4. Strain rate dependence of true stress ($\varepsilon = 0.29$, corresponding to the steady flow) for the alloy tested.

plotted. Figure 3a exhibits the true stress–true strain behavior for the alloy under the condition of constant crosshead speed while Fig. 3b exhibits the true stress–true strain behavior under the condition of constant strain rate.

From curve (1) in Fig. 3b, we can observe that at high strain rate, the true stress–true strain curves exhibit a modest increase after yield, followed by a rapid decrease of stress. Curve (2) in Fig. 3b shows that as the strain rate decreases, the flow stress decreases. Corresponding to this variation, the steady flow extends to a large strain without fracture, being typical for many superplastic materials [12, 13]. However, at slow strain rate, the true stress–true strain curves exhibit a continuous increase untill fracture (curve (3) in Fig. 3b). The influence of temperature is similar to the influence of strain rate, an increase of temperature leads to the same pattern in the stress-strain curves as that observed by a decrease in strain rate.

3.3. Constitutive equation

High temperature deformation of materials under steady-state conditions can be generally expressed by the relation between flow stress (σ) and strain rate ($\dot{\varepsilon}$):

$$\dot{\varepsilon} = A\sigma^n \exp(-Q/RT) \tag{2}$$

where A is a constant, n is the stress exponent being equal to $1/m$ (m is the strain rate sensitivity index), Q is the apparent activation energy, R is the gas constant and T is the thermodynamic temperature. Figure 4 shows the relationship between the flow stress ($\varepsilon = 0.29$) and the strain rate for the alloy at various temperatures, which can be divided into two regions. Linear relationships are found for the alloy when the strain rate is higher than $1.04 \times 10^{-3}\ s^{-1}$ with the strain rate sensitivity index $m = 0.30$, while the strain rate sensitivity index attains 0.50 when the strain rate is lower than $1.04 \times 10^{-3}\ s^{-1}$.

From Eq. (2) it can be shown that:

$$Q = n \cdot R \cdot \frac{\partial \ln \sigma}{\partial (1/T)} \tag{3}$$

where $n = 1/m$. Figure 5 shows an Arrhenius plot for the flow stress of the tested alloy where the stresses corresponding to the steady flow in the true stress–true strain curves were used as the flow stress. The plot is performed for strain rates of $5.20 \times 10^{-4}\ s^{-1}$ ($n = 2$) and $5.20 \times 10^{-3}\ s^{-1}$ ($n = 3$). The apparent activation energy is calculated to be about 143 kJ mol^{-1} and 324 kJ mol^{-1} based on the Eq. (2). The activation energy value for strain rates of $5.20 \times 10^{-4}\ s^{-1}$ is about half of the value (~ 220–300 kJ mol^{-1}) measured for the creep deformation of NiAl, while for the strain rate of $5.20 \times 10^{-3}\ s^{-1}$, the apparent activation energy is more than the value measured for the creep deformation of NiAl [1]. This indicates that different deformation mechanisms are operative at different strain rate regions.

3.4. Microstructural observation

Figure 6 shows an SEM image of the specimen with a strain of 0.8 tested at 1323 K under an initial strain rate of $1.04 \times 10^{-4}\ s^{-1}$. The grains of primary NiAl matrix in the gage section have significantly coarsened with a mean grain

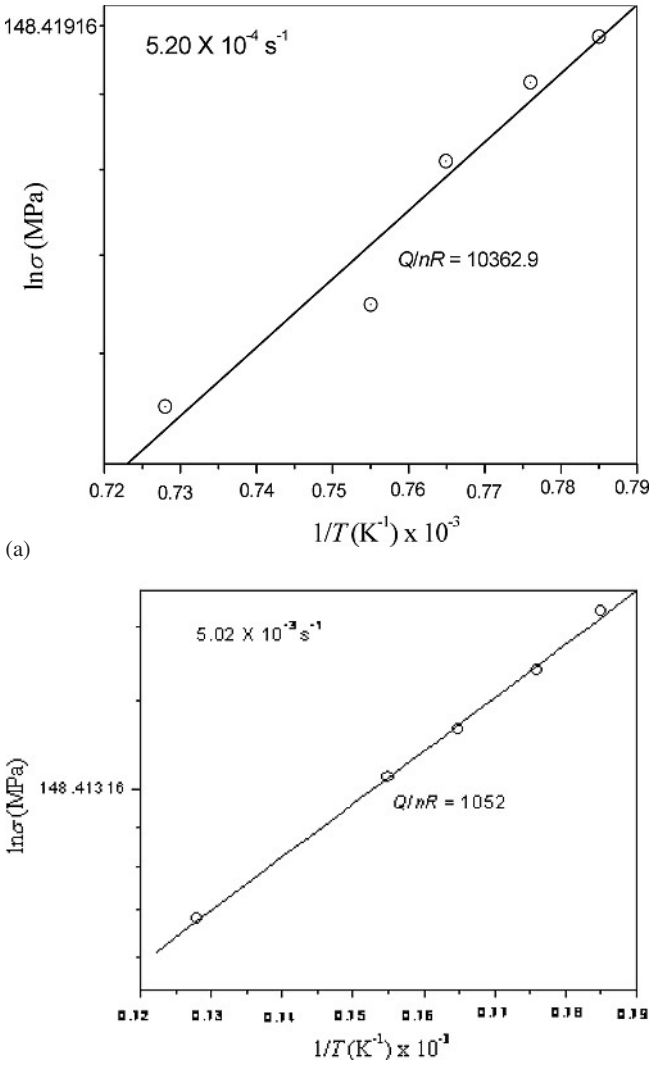

Fig. 5. The Arrhenius plot for the alloy in two deformation regions.

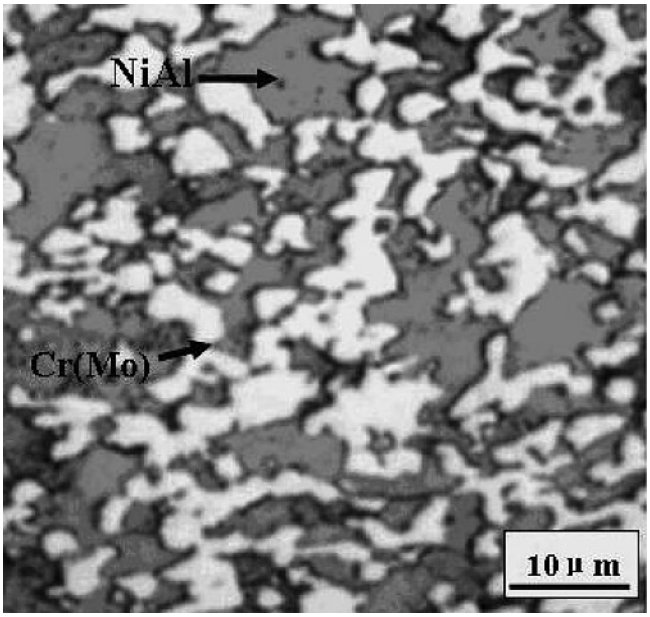

Fig. 6. The SEM observation of microstructure evolution of the alloy deforming at 1323 K under the strain rate of $1.04 \times 10^{-4}\ s^{-1}$.

size of more than 10 μm. The coarsening may explain the continuous strain hardening behavior for the alloy deforming under the above conditions, as shown in Fig. 3b. Cr(Mo) phase is slightly elongated towards the tensile direction after superplastic deformation. This shows that Cr(Mo) phase has deformed and provided some strain to the alloy during superplastic deformation process.

Figure 7 shows TEM observations of the specimens obtained at different strains corresponding to the strain region of continuous working hardening flow deforming at 1323 K under an initial strain rate of $1.04 \times 10^{-4}\ s^{-1}$. Figure 7a shows a high density of dislocations around grain boundaries of the NiAl matrix at a strain of 0.70. These dislocations are thought to be introduced to accommodate stress generated by grain boundary sliding. Figure 7b shows that the dislocations demonstrate the tendency to form tangles of dislocations and a dislocation wall has almost formed, indicating that a dynamic recovery process has occurred during the superplastic deformation process.

4. Discussion

Now we can discuss the mechanisms of the elevated-temperature deformation of the present as-HIPped alloy based on both mechanical and metallographic observations. It is known that the plastic flow of metallic alloys arises from two independent processes at high temperatures [16]. In one process GBS accommodated by dislocation behavior occurs in the boundary region, and in the other dislocation slip or diffusion occurs within the core of each grain. Due to the fact that the stress exponent n measured under the strain rates lower than $1.04 \times 10^{-3}\ s^{-1}$ at 1323 K and 1373 K in this work was about 2.0, the mechanisms associated with dislocation slip or diffusional creep may be excluded [16]. In fact, under strain rates lower than $1.04 \times 10^{-3}\ s^{-1}$ at more than 1323 K, a high m value of 0.5 implies that grain boundary sliding is occurring at grain boundaries between NiAl and adjacent NiAl or Cr(Mo) grains; this trend is also noted in other superplastic materials [14, 15]. The apparent energy for the high temperature deformation of the alloy at this strain rate regime is calculated as 143 kJ mol^{-1}, which is close to a half of the activation energy of the bulk diffusion of NiAl (220–300 kJ mol^{-1}) [1]. Therefore, it is suggested that grain boundary diffusion of the NiAl matrix is involved in the superplastic deformation process.

Now that the mechanism for the superplastic flow involves grain boundary sliding, it is necessary for an accommodation process to accompany grain boundary sliding. TEM observations (Fig. 6) have shown that there existed a high density of dislocations around interfaces of NiAl and Cr(Mo), although the equiaxed structure of NiAl is still maintained. A resonable explanation of high dislocation density areas near the interface is that they are produced by boundaries sliding between NiAl and Cr(Mo) phases. That is, these dislocations will be introduced to accommodate stress generated by boundaries sliding between NiAl and adjacent NiAl or Cr(Mo) grains.

From Fig. 7b, we know that that a dynamic recovery process has occurred during the superplastic deformation process. The dynamic recovery process is closely related to the ease of dislocation glide and climb in NiAl grains. Many experiments have shown that dislocations in the pri-

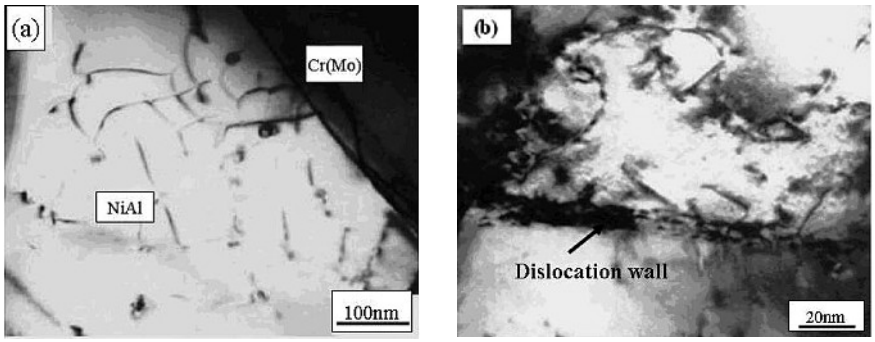

Fig. 7. TEM observations of the specimens obtained at different strains (a) $\varepsilon = 0.70$; (b) $\varepsilon = 1.40$ at 1323 K under an initial strain rate of $1.04 \times 10^{-4}\ s^{-1}$.

mary NiAl matrix are operative (slide and climb) by TEM images. For example, Lautenschlager et al. [17] had predicted that {100}<100>, {110} <100> and {110}<110> are operative in NiAl deformed at high temperature, by limited slip trace investigations. It is generally believed that in ordered intermetallics, dislocations glide in the form of superdislocations, i.e., a pair of unit dislocations connected by a planar fault. The high stacking fault energy of the B2 NiAl alloy forces the activated dislocation to easily shrink and climb instead of splitting into partials at elevated temperature [1, 2]. As a result, under the combined operation of slide and climb of dislocation, a dynamic recovery process may occur for the alloy during deformation at high temperatures. Some authors have proposed an operative process of dynamic recovery in B2 type intermetallic materials during the high-temperature deformation process [18]. During the dynamic recovery process, dislocations in the grains can be attracted and absorbed by a dislocation line even sub-boundary. Therefore, the dynamic recovery process can effectively absorb deformation energy and then accommodate the stress concentration from grain boundaries sliding.

In terms of the accommodation process, the grain boundary sliding-based mechanism has been divided into two kinds of concept by considering "local" and "long range" accommodation at or near grain boundaries [19]. Local accommodation can be done by the motion of run-in and run-out dislocations. On the other hand, there are three detailed proposed mechanisms dealing with long range accommodation at triple points. Both grain boundary sliding-based mechanisms with local and long range accommodation lead to a stress index of $n = 2$. The n value observed in the superplastic deformation of the alloy is about 2. Furthermore, the activations and motions of dislocations are actually observed near the grain boundary. These experimental results indicate that the grain boundaries sliding accommodated by the operation of run-in or run-out dislocations (i.e., local accommodation) is very likely.

5. Conclusions

The superplastic deformation behavior of hot isostatic pressed (HIPped) NiAl-28Cr-6Mo doped with Dy fabricated through spray forming has been characterized. The conclusions can be given as follow:

(1) The material obtained exhibits superplastic deformation at a strain rate range ($\sim 10^{-3}\ s^{-1} - 10^{-4}\ s^{-1}$) above 1323 K with an m value of 0.5.
(2) NiAl grains remain almost equiaxed after superplastic deformation. TEM observations show that a high density of dislocations near grain boundaries even the dislocation wall has been observed in NiAl phase.
(3) Based on the mechanical and microstructural observations, it is suggested that the grain boundaries slide between NiAl and adjacent NiAl or Cr(Mo) grains with local range accommodation, i.e., dynamic recovery is responsible for the superplastic deformation of the HIP alloy.

References

[1] B. Miracle: Acta Metall. Mater. 41 (1993) 649.
[2] D. Noebe, R. Bowman, V. Nathal: NASA technical paper. April (1994) 3398.
[3] R. Johnson, F. Chen, F. Oliver, D. Noebe, D. Whittenberger: Intermetallics 3 (1995) 99.
[4] R. Johnson, F. Oliver, D. Noebe, D. Whittenberger: Intermetallics 3 (1995) 493.
[5] Y. Sakka, T. Matsumoto, S. Atsumo, S. Suzuki: Adv. Eng. Mater. 5 (2003) 130.
[6] X.H. Du, J.T. Guo, B.D. Zhou: Scr. Mater. 45 (2001) 69.
[7] J.T. Guo, X.H. Du: Intermetallics 13 (2005) 257.
[8] D. Jiang, D. Lin: Mater. Let. 57 (2004) 747.
[9] L. Dongliang, H. Jing, J. Dongmei: Intermetallics 13 (2005) 343.
[10] J.T. Guo, X.H. Du, B.D. Zhou. Intermetallics 10 (2002) 435.
[11] R.S. Chen, J.T. Guo, W.M. Yin, J.Y.Zhou: Scr. Mater. 40 (1999) 209.
[12] W.L. Zhou, J.T. Guo, R.S. Chen, J.Y. Zhou: Mater. Let. 47 (2001) 30.
[13] T. Oomori, T. Yoneyama, H. Oikama: Trans. JIM 29 (1988) 399.
[14] O.D. Sherby, J. Wadsworth: Prog. Mater. Sci. 33 (1989) 169.
[15] T.G. Nieh, J. Wadsworth: Inter. Mater. Rev. 44 (1999) 59.
[16] R.L. Coble: J. Appl. Phys. 34 (1963) 1679.
[17] E.P. Lautenschlager, T.C. Tisone: Phys. Stat. Sol. 20 (1973) 443.
[18] X.H. Du, J.T. Guo, L.Z. Zhou: Mater. Sci. Tech. 20 (2004) 82.
[19] T. Takasugi, S. Rikukawa, S. Hanada: Acta Metall. Mater. 40 (1992) 1895.

(Received ■; accepted ■)

Correspondence address

J. C. Huang
Institute of Materials Science and Engineering
Center for Nanoscience and Nanotechnology
National Sun Yat-San University
Kaohsiung 804, Taiwan, Republik of China
Tel.: +886 7 525 2000 x 4063
Fax: +886 7 525 4099
E-mail: jacobc@mail.nsysu.edu.tw